PHILOSOPHICAL TRANSACTIONS OF THE ROYAL SOCIETY A MATHEMATICAL, PHYSICAL & ENGINEERING SCIENCES

Bonding and Structure of Intermetallics: A New Bond Order Potential [and Discussion]

D. G. Pettifor, M. Aoki, J. N. Murrell, A. Cottrell and A. M. Stoneham

Phil. Trans. R. Soc. Lond. A 1991 **334**, 439-449
doi: 10.1098/rsta.1991.0024

Bonding and structure of intermetallics: a new bond order potential

By D. G. Pettifor and M. Aoki

Department of Mathematics, Imperial College of Science, Technology and Medicine, London SW7 2BZ, U.K.

Intermetallics such as the transition metal aluminides present theorists with a challenge since bonding is not well described by currently available pair or embedded atom potentials. We show that a new angularly dependent, many-body potential for the bond order has all the necessary ingredients for an adequate description. In particular, by linearizing the moment-recursion coefficient relations, a cluster expansion is derived which is applicable to any lattice and chemical ordering and which allows a derivation of the earlier ring ansatz. It can account for both the negative Cauchy pressure of cubic metals and the oscillatory behaviour across the transition metal aluminide series of the three-body cluster interaction Φ_3.

1. Introduction

Intermetallics have come to the fore during the past few years with the realization that polycrystalline Ni_3Al could be ductilized by adding very small amounts of boron (Aoki & Izumi 1979). The search for new intermetallics for use at high temperatures, in jet engines for example, has focused on the transition metal aluminides which are often both light and oxidation resistant (Dimiduk & Miracle 1989). In particular, alloy designers have been interested in whether it is possible to ductilize the tri-aluminides Al_3T by alloying so that their crystal structure changed from tetragonal (and brittle) to cubic (and hopefully ductile).

Structure maps, which order the known structural data base on binary compounds within a limited number of two-dimensional or three-dimensional plots, can provide a useful guide in the search for new pseudo-binary alloys with a required structure type (Pettifor 1991). Figure 1 shows the relevant part of the AB_3 structure map which has ordered 'the wood from the trees' by characterizing each element in the periodic table with a single phenomenological coordinate, called the Mendeleev number $\mathscr{M}$ (Pettifor 1988). We see that the intermetallics Al_3Hf, Al_3Ti, Al_3Ta, Al_3Nb, and Al_3V with Mendeleev numbers ranging from $\mathscr{M}_A$ equals 50 to 53 respectively all fall within the tetragonal DO_{22} domain. It was known that Al_3Ti could be stabilized in the cubic $L1_2$ crystal structure by replacing some of the aluminium with Cu, Ni, or Fe. The structure map suggests that it might be possible to stabilize the other tetragonal tri-aluminides in the cubic crystal structure by alloying so that the average Mendeleev number for the B sites moves down into the cubic $L1_2$ domain.

This hope has only been partially realized. Schneibel & Porter (1989) have indeed succeeded in stabilizing cubic Al_3Zr by alloying to take the average Mendeleev number $\bar{\mathscr{M}}_B$ down into the cubic domain. However, attempts to stabilize cubic Al_3Nb

Phil. Trans. R. Soc. Lond. A (1991) **334**, 439–449
Printed in Great Britain

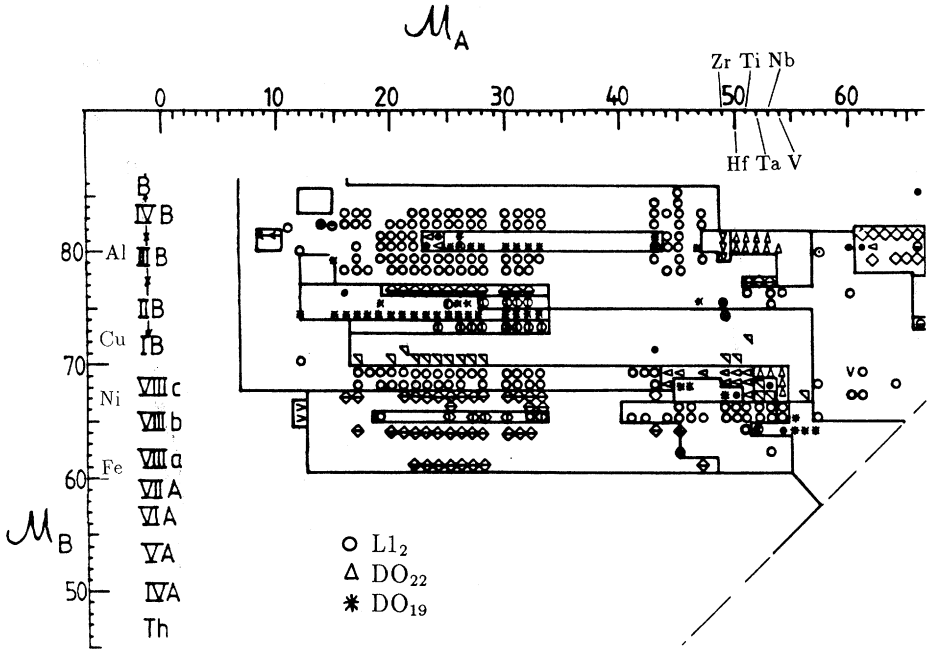

Figure 1. Relevant part of the AB_3 structure map showing the transition metal tri-aluminides. (After Nicholson *et al.* 1989.)

have failed (Subramanian *et al.* 1989). Moreover, the cubic tri-aluminides based on Al_3Zr and Al_3Ti still remain brittle, cleaving transgranularly, even though they have the same crystal structure as ductile single crystals of Cu_3Au or Ni_3Al. Theorists, are, therefore, faced with two immediate problems regarding the transition metal tri-aluminides: (i) Why if the cubic close-packed phase can be stabilized, does it remain brittle? (ii) Why can some tetragonal tri-aluminides be stabilized in the cubic form (e.g. Al_3Ti) but others cannot (e.g. Al_3Nb)? We shall see that the answer to both questions requires a proper quantum mechanical treatment of the bonding at the atomistic level.

2. A new bond order potential

A clue to the origin of the brittleness of the cubic transition metal tri-aluminides is provided by their elastic constants. Fu (1991) has recently calculated within first principles local density functional theory that cubic Al_3Ti has a Cauchy pressure $C_{12}-C_{44}$ of -0.08×10^{11} N m^{-2}, which is to be compared with a Cauchy pressure of $+0.13\times10^{11}$ N m^{-2} for Ni_3Al. This has important consequences for the nature of the bonding at the atomistic level. If the bonding is describable by nearest-neighbour pairwise potentials such as Lennard-Jones, then the Cauchy pressure would be zero. If the bonding is more metallic in that spherical atoms are embedded in the electron gas of the surrounding neighbours, then the Cauchy pressure would be positive (Johnson 1988). A negative Cauchy pressure puts cubic Al_3Ti in the same class as the four-fold coordinated semi-conductor Si with a $C_{12}-C_{44}$ of -0.16×10^{11} N m^{-2}. This implies that angularly dependent many-body forces are playing a crucial role in the transition metal tri-aluminides.

Recently a new many-body potential for the bond order has been proposed which explicitly includes the angular character of the bonding orbitals (Pettifor 1989,

1990). It is derived from tight binding Hückel theory in which the quantum mechanical bond energy between a given pair of atoms i and j is written in the chemically intuitive form as follows:

$$U^{ij}_{\text{bond}} = 2h(R_{ij})\,\Theta_{ij}, \tag{2.1}$$

where $h(R_{ij})$ is the appropriate σ, π or δ bond integral between atoms i and j a distance R_{ij} apart (see eqs (65) and (80) of Pettifor (1990)) and Θ_{ij} is the corresponding bond order which is defined as the difference between the number of electrons of a given spin in the bonding $\frac{1}{\sqrt{2}}|\phi_i+\phi_j\rangle$ and anti-bonding $\frac{1}{\sqrt{2}}|\phi_i-\phi_j\rangle$ states. The factor 2 in equation (2.1) accounts for spin degeneracy. The bonding between any given pair of atoms will, of course, be weakened by the presence of bonds with other neighbouring atoms. Thus the bond order is not pairwise but is dependent on the surrounding atomic environment.

Its analytic dependence may be obtained by using the recursion method of Haydock *et al.* (1972) to write the bond order as an integral over the difference of two continued fractions:

$$\Theta_{ij} = -\frac{1}{\pi}\,\text{Im}\int^{E_F}[G^+_{00}(E)-G^-_{00}(E)]\,\mathrm{d}E, \tag{2.2}$$

where E_F is the Fermi energy and Im is the imaginary part of the bonding and antibonding Green's functions which are given by

$$\begin{aligned} G^{\pm}_{00}(E) &= \langle u^{\pm}_0|(E-H)^{-1}|\,u^{\pm}_0\rangle \\ &= \cfrac{1}{(E-a^{\pm}_0)-(b^{\pm}_1)^2/(E-a^{\pm}_1)-\ldots}, \end{aligned} \tag{2.3}$$

where $|u^{\pm}_0\rangle = \frac{1}{\sqrt{2}}|\phi_i \pm \phi_j\rangle$. The coefficients are determined by the Lanczos recursion algorithm, namely

$$b^{\pm}_{n+1}|u^{\pm}_{n+1}\rangle = H\,|u^{\pm}_n\rangle - a^{\pm}_n\,|u^{\pm}_n\rangle - b^{\pm}_n\,|u^{\pm}_{n-1}\rangle \tag{2.4}$$

with the boundary condition that $|u^{\pm}_{-1}\rangle$ vanishes. The hamiltonian H is, therefore, tridiagonal with respect to the recursion basis $|u^{\pm}_n\rangle$, having non-zero elements

$$\langle u^{\pm}_n|\,H\,|u^{\pm}_n\rangle = a^{\pm}_n \tag{2.5}$$

and

$$\langle u^{\pm}_{n+1}|\,H\,|u^{\pm}_n\rangle = b^{\pm}_{n+1}. \tag{2.6}$$

Thus the hamiltonian with respect to the bonding and antibonding recursion basis may be characterized by the semi-infinite linear chain with site diagonal elements $a^{\pm}_n$ and intersite hopping matrix elements $b^{\pm}_{n+1}$, namely

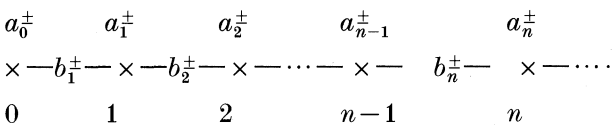

A many-body form for the bond order may be derived by performing perturbation theory with respect to the average semi-infinite linear chain, namely

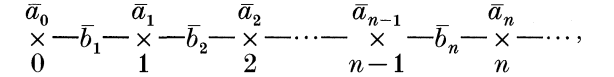

where $\bar{a}_n = \frac{1}{2}(a_n^+ + a_n^-)$ and $\bar{b}_n = \frac{1}{2}(b_n^+ + b_n^-)$. It follows from the first-order Dyson equation that

$$G_{00}^{\pm} = G_{00}^0 \pm \sum_{n=0}^{\infty} G_{0n}^0 G_{n0}^0 \,\delta a_n \pm 2 \sum_{n=1}^{\infty} G_{0(n-1)}^0 G_{n0}^0 \,\delta b_n, \tag{2.7}$$

where $\delta a_n = \frac{1}{2}(a_n^+ - a_n^-)$, $\delta b_n = \frac{1}{2}(b_n^+ - b_n^-)$, and G^0 is the Green's function for the average semi-infinite linear chain. Substituting into (2.2) the bond order becomes

$$\Theta = -2\left[\sum_{n=0}^{\infty} \chi_{0n,\,n0}(E_{\mathrm{F}})\,\delta a_n + 2\sum_{n=1}^{\infty} \chi_{0(n-1),\,n0}(E_{\mathrm{F}})\,\delta b_n\right], \tag{2.8}$$

where the response functions $\chi_{0m,\,n0}(E_{\mathrm{F}})$ are defined by

$$\chi_{0m,\,n0}(E_{\mathrm{F}}) = \frac{1}{\pi}\,\mathrm{Im}\int^{E_{\mathrm{F}}} G_{0m}^0(E)\,G_{n0}^0(E)\,\mathrm{d}E. \tag{2.9}$$

The coefficients δa_n, δb_n may be written in terms of the local topology about the bond by using the well-known relationship between the recursion coefficients $a_n^{\pm}$, $b_n^{\pm}$ and the moments $\mu_n^{\pm} = \langle u_0^{\pm}|H^n|\,u_0^{\pm}\rangle$, namely

$$\mu_0^{\pm} = 1, \tag{2.10}$$

$$\mu_1^{\pm} = a_0^{\pm}, \tag{2.11}$$

$$\mu_2^{\pm} = (a_0^{\pm})^2 + (b_1^{\pm})^2, \tag{2.12}$$

$$\mu_3^{\pm} = (a_0^{\pm})^3 + 2a_0^{\pm}(b_1^{\pm})^2 + a_1^{\pm}(b_1^{\pm})^2, \tag{2.13}$$

$$\mu_4^{\pm} = (a_0^{\pm})^4 + 3(a_0^{\pm})^2(b_1^{\pm})^2 + 2a_0^{\pm}a_1^{\pm}(b_1^{\pm})^2 + (a_1^{\pm})^2(b_1^{\pm})^2 + (b_1^{\pm})^2(b_2^{\pm})^2 + (b_1^{\pm})^4 \tag{2.14}$$

and

$$\begin{aligned}\mu_5^{\pm} = {} & (a_0^{\pm})^5 + 4(a_0^{\pm})^3(b_1^{\pm})^2 + 3(a_0^{\pm})^2 a_1^{\pm}(b_1^{\pm})^2 \\ & + 3a_0^{\pm}(b_1^{\pm})^4 + 2a_0^{\pm}(a_1^{\pm})^2(b_1^{\pm})^2 + 2a_0^{\pm}(b_1^{\pm})^2(b_2^{\pm})^2 \\ & + 2a_1^{\pm}(b_1^{\pm})^4 + 2a_1^{\pm}(b_1^{\pm})^2(b_2^{\pm})^2 + (a_1^{\pm})^3(b_1^{\pm})^2 \\ & + a_2^{\pm}(b_1^{\pm})^2(b_2^{\pm})^2.\end{aligned} \tag{2.15}$$

The difference between the bonding and antibonding moments may be displayed explicitly by writing

$$\mu_n^{\pm} = \mu_n \pm \zeta_{n+1}, \tag{2.16}$$

where it follows that since $|u_0^{\pm}\rangle = \frac{1}{\sqrt{2}}|\phi_i + \phi_j\rangle$ we have that μ_n is the average nth moment with respect to the appropriate orbitals on site i and j, namely

$$\mu_n = \tfrac{1}{2}[\langle\phi_i|H^n|\,\phi_i\rangle + \langle\phi_j|H^n|\,\phi_j\rangle] = \tfrac{1}{2}(\mu_n^i + \mu_n^j) \tag{2.17}$$

and ζ_{n+1} is the interference term, namely

$$\zeta_{n+1} = \langle\phi_i|H^n|\,\phi_j\rangle. \tag{2.18}$$

The interference terms control the bond order which can be seen using the moment expansion for $G^{\pm}$, namely

$$G^+(Z) - G^-(Z) = \sum_{n=0}^{\infty} \frac{\mu_n^+ - \mu_n^-}{Z^{n+1}} = 2\sum_{n=1}^{\infty} \frac{\zeta_{n+1}}{Z^{n+1}}. \tag{2.19}$$

However, the moment expansion is notoriously ill conditioned. We, therefore, rewrite the stable recursion expansion for the bond order, equation (2.8), in terms of the ζ_{n+1} by linearizing the moment-recursion coefficient relations in equations (2.10)–(2.15). We find to first order in $\zeta_{n+1}/\mu_2^{n/2}$, taking $\bar{a}_0 = \mu_1 = 0$ as the reference energy, that the average recursion coefficients $\bar{a}_n, \bar{b}_n$ are given by

$$\bar{a}_0 = \mu_1 \equiv 0, \tag{2.20}$$

$$\bar{b}_1 = \mu_2^{\frac{1}{2}}, \tag{2.21}$$

$$\bar{a}_1 = \mu_3/\mu_2, \tag{2.22}$$

$$\bar{b}_2 = (\mu_4/\mu_2 - \mu_3^2/\mu_2^2 - \mu_2)^{\frac{1}{2}}, \tag{2.23}$$

and

$$\bar{a}_2 = [\mu_5 - 2\mu_3(\mu_4/\mu_2 - \mu_3^2/\mu_2^2) - \mu_3^3/\mu_2^2]/(\bar{b}_1)^2\,(\bar{b}_2)^2. \tag{2.24}$$

That is, to first order, the average coefficients $\bar{a}_n, \bar{b}_n$, which enter the reference response functions $\chi_{0m,\,n0}(E_{\mathrm{F}})$, are determined solely by the average moments μ_n which characterize the average Green's function associated with the appropriate orbitals on sites i and j, namely

$$\bar{G}(E) = \tfrac{1}{2}[G_{ii}(E) + G_{jj}(E)]. \tag{2.25}$$

The coefficients $\delta a_n, \delta b_n$, on the other hand, are given to first order in ζ_{n+1} by

$$\delta a_0 = \zeta_2 \equiv \langle \phi_i | H | \phi_j \rangle, \tag{2.26}$$

$$\delta b_1 = \zeta_3/(2\mu_2^{\frac{1}{2}}), \tag{2.27}$$

$$\delta a_1 = \zeta_4/\mu_2 - (\mu_3/\mu_2^2)\,\zeta_3 - 2\zeta_2, \tag{2.28}$$

$$\delta b_2 = [\zeta_5 - (2\mu_3/\mu_2)\,\zeta_4 - (\mu_4/\mu_2 - 2\mu_3^2/\mu_2^2 + \mu_2)\,\zeta_3 + 2\mu_3\,\zeta_2]/[2(\bar{b}_1)^2\,\bar{b}_2], \tag{2.29}$$

and

$$\begin{aligned}\delta a_2 = \Bigg\{ & \zeta_6 - \frac{\mu_5 - 2\mu_2\mu_3 - \mu_3^3/\mu_2^2}{(\bar{b}_1)^2\,(\bar{b}_2)^2}\,\zeta_5 \\ & - \left[\frac{2\mu_4}{\mu_2} + \frac{\mu_3^2}{\mu_2^2} + \frac{4\mu_3^2}{\mu_2\,\bar{b}_2^2} + \frac{2\mu_3^4}{\mu_2^4(\bar{b}_2)^2} - \frac{2\mu_3\mu_5}{\mu_2^2(\bar{b}_2)^2}\right]\zeta_4 \\ & - \left[\frac{\mu_5}{\mu_2} - \frac{\mu_3^3}{\mu_2^3} - \frac{2\mu_3\mu_4}{\mu_2^2} + \left(\frac{\mu_4}{\mu_2} - \frac{2\mu_3^2}{\mu_2^2} + \mu_2\right)\left(\frac{\mu_3^3}{\mu_2^3(\bar{b}_2)^2} + \frac{2\mu_3}{(\bar{b}_2)^2} - \frac{\mu_5}{\mu_2(\bar{b}_2)^2}\right) + 2\mu_3\right]\zeta_3 \\ & - \left[\frac{2\mu_3\mu_5}{\mu_2(\bar{b}_2)^2} + \mu_2^2 - 2\mu_4 - \frac{2\mu_3^2}{\mu_2} - \frac{2\mu_3^4}{\mu_2^3\,\bar{b}_2^2} - \frac{4\mu_3^2}{(\bar{b}_2)^2}\right]\zeta_2\Bigg\} \Bigg/ [(\bar{b}_1)^2\,(\bar{b}_2)^2].\end{aligned} \tag{2.30}$$

The coefficients $\delta a_n, \delta b_n$ take a particularly transparent form if we assume that $\bar{b}_2 = \bar{b}_1$ and $\mu_{2n+1}/\mu_2^{(2n+1)/2} \ll 1$. It then follows from equations (2.26)–(2.30) that

$$\delta a_0 = \zeta_2, \tag{2.31}$$

$$2\delta b_1 = \zeta_3/\mu_2^{\frac{1}{2}}, \tag{2.32}$$

$$\delta a_1 = (\zeta_4 - 2\mu_2\,\zeta_2)/\mu_2, \tag{2.33}$$

$$2\delta b_2 = (\zeta_5 - 3\mu_2\,\zeta_3)/\mu_2^{\frac{3}{2}}, \tag{2.34}$$

and

$$\delta a_2 = [\zeta_6 - 4\mu_2(\zeta_4 - 2\mu_2\,\zeta_2) - \mu_2^2\,\zeta_2 - 2\mu_4\,\zeta_2]/\mu_2^2. \tag{2.35}$$

The ζ_n can be represented diagrammatically as in figure 2. The first diagram

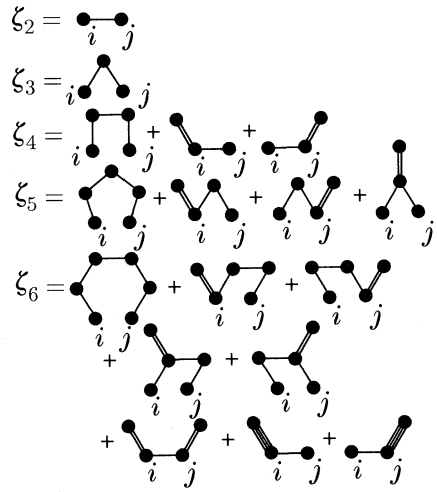

Figure 2. Diagrammatic representation of the interference terms ζ_n between atoms i and j.

represents the ring term ζ_n^r in which all n sites are distinct and there are no self-retracing paths, whereas the latter diagrams are dressed by self-retracing paths which must be summed over all nearest neighbour sites. We have neglected double-counting terms which involve hopping backwards and forwards between atoms i and j. This is a good approximation for s orbitals on lattices with large local coordination z as the hops to the z nearest neighbours swamp the double-counting contribution. It follows from equations (2.31)–(2.35) that the dressed diagrams cancel from the $\delta a_n, \delta b_n$, leaving only the ring terms, namely

$$\delta a_0 = \zeta_2^r, \tag{2.36}$$

$$\delta b_1 = \zeta_3^r / 2\mu_2^{\frac{1}{2}}, \tag{2.37}$$

$$\delta a_1 = \zeta_4^r / \mu_2, \tag{2.38}$$

$$\delta b_2 = \zeta_5^r / 2\mu_2^{\frac{3}{2}}, \tag{2.39}$$

and

$$\delta a_2 = \zeta_6^r / \mu_2^2. \tag{2.40}$$

The response functions consistent with equations (2.36)–(2.40), which were derived by neglecting odd moments and taking $\bar{b}_2 = \bar{b}_1$, are those corresponding to a reference semi-infinite linear chain with $\bar{a}_n = 0$, $\bar{b}_n = \bar{b}_1 \equiv b$. They may be written (Pettifor 1989) as $\chi_{0m,n0} = \hat{\chi}_{m+n+2}/|b|$ for $m = n-1$ or n where the reduced susceptibility

$$\hat{\chi}_{m+n+2}(N) = \frac{1}{\pi}\left[\frac{\sin(m+n+1)\,\phi_F}{m+n+1} - \frac{\sin(m+n+3)\,\phi_F}{m+n+3}\right] \tag{2.41}$$

with $\phi_F = \arccos(E_F/2b)$. ϕ_F is fixed by the number of valence electrons per spin per bond, N, through

$$N = (2\phi_F/\pi)\,[1-(\sin 2\phi_F)/2\phi_F]. \tag{2.42}$$

Figure 3 shows the behaviour of the first five reduced response functions $\hat{\chi}_n$ as a function of the number of valence electrons per spin per bond. We see that the number of nodes (excluding the end points) equals $(n-2)$.

Figure 3

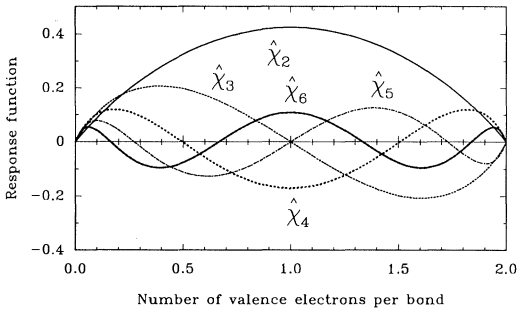

Figure 4

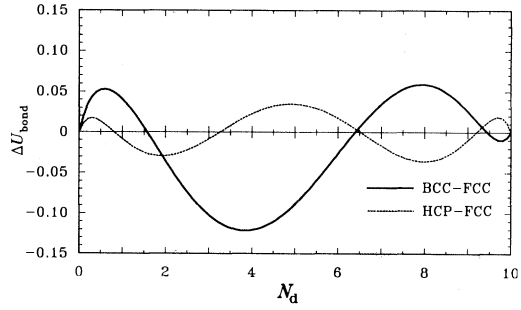

Figure 3. The reduced response functions $\hat{\chi}_n$ as a function of the number of valence electrons per spin per bond N.

Figure 4. The total bond energy difference (in units of band width) between BCC, HCP, and FCC transition metals as a function of the number of valence d electrons per atom N_d for the BCC lattice.

We shall refer to the use of equations (2.36)–(2.41) as the ring approximation (RA), in which the bond order is written

$$\Theta = 2 \sum_{n=2}^{\infty} \hat{\chi}_n(N)\, \zeta_n^r / b^{n-1}. \tag{2.43}$$

Elsewhere we have used the RA potential to investigate the relative stability of linear, square, or tetrahedral s-valent clusters (Pettifor 1989) and the angular character of the embedding function b for sp- and sd-valent systems (Pettifor 1990). Here we demonstrate that it reproduces the observed trends in crystal structure and elastic constants across the transition metal series.

Figure 4 shows the total bond energy difference between the BCC, HCP, and FCC lattices as a function of the number of valence d electrons per atom, retaining the first five terms in (2.43). We seen that it shows the well-known trend from HCP → BCC → HCP → FCC(→ BCC) across the non-magnetic 4d and 5d series (see, for example, fig. 35 of Pettifor (1983)). The BCC stability for nearly half-full bands is associated with the four-membered ring term through $\hat{\chi}_4$, the cubic versus hexagonal stability with the six-membered ring term through $\hat{\chi}_6$.

Figure 5 shows the behaviour of the Cauchy pressure $C_{12} - C_{44}$ as a function of the number of valence d electrons per atom for the BCC lattice. We see that it oscillates in sign, so that the RA potential (unlike pair or embedded atom potentials) can account naturally for the negative Cauchy pressures of brittle metals such as elemental FCC Ir or the cubic pseudo-binary intermetallic Al_3Ti. It remains to fit RA potentials to these specific systems and to model the behaviour of their defects such as dislocation cores or crack tips atomistically. In another publication (Aoki & Pettifor 1991) we present analytic expressions for the response functions beyond the RA and examine in detail the convergence of the bond order series equation (2.8) and the accuracy of linearizing the moment-recursion coefficient relations equations (2.10)–(2.15).

3. Two- and three-body cluster interactions

The linearized bond order potential can also shed light on why some tetragonal tri-aluminides can be stabilized in the cubic form (e.g. Al_3Ti) but others cannot (e.g. Al_3Nb). Carlsson (1989) has recently used the Connolly–Williams method to find the

Figure 5

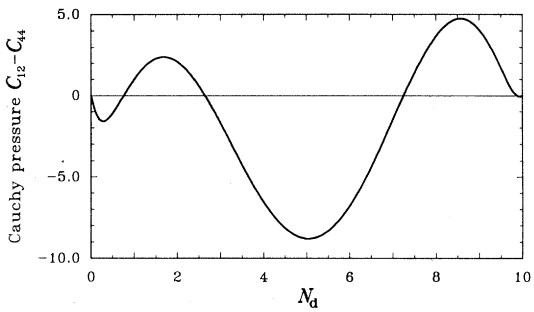

Figure 6

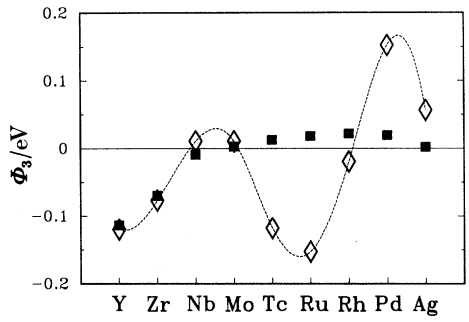

Figure 5. The Cauchy pressure $C_{12}-C_{44}$ as a function of the number of valence d electrons per atom N_d for the BCC lattice.

Figure 6. The three-body cluster interaction Φ_3 for the 4d transition metal aluminides (after Carlsson 1989). The squares denote the predictions of Miedema's model.

effective interaction parameters in a cluster expansion for the total binding energy of FCC-based transition metal aluminides, namely

$$U = \Phi_0 + \Phi_1\langle\sigma_i\rangle + \Phi_2\langle\sigma_i\sigma_j\rangle + \Phi_3\langle\sigma_i\sigma_j\sigma_k\rangle + \Phi_4\langle\sigma_i\sigma_j\sigma_k\sigma_l\rangle. \tag{3.1}$$

Here σ_i is a spin-like variable which takes the value 1 and -1 for transition and aluminium atoms respectively. The averages are taken over all sites, nearest-neighbour pairs, nearest-neighbour triangles, and nearest-neighbour tetrahedra.

The heat of formation for the disordered transition metal aluminide T_cAl_{1-c} is then given by

$$\Delta H^{\mathrm{dis}}(c) = -4c(1-c)\,[\Phi_2 - (1-2c)\,\Phi_3 + 2(1-2c+2c^2)\,\Phi_4]. \tag{3.2}$$

We see that regular solution behaviour is determined by the two-body cluster interaction Φ_2, whereas the skewing of the heat of formation curve is determined by the three-body cluster interaction Φ_3. Carlsson's (1989) local density functional calculations predict that Φ_3 oscillates across the transition metal aluminide series as shown for the 4d series in figure 6. For $\Phi_3 < 0$ the parabolic regular solution curve is skewed towards the aluminium rich end, whereas for $\Phi_3 > 0$ the curve is skewed towards the transition metal rich end. Thus figure 6 predicts that FCC-based Al_3Zr (or Al_3Ti) will be more stable than FCC-based $AlZr_3$ (or $AlTi_3$), whereas FCC-based Al_3Nb (or Al_3V) will be less stable than FCC-based $AlNb_3$ (or AlV_3). It is, thus, not surprising that Al_3Ti can be stabilized in the cubic $L1_2$ form but Al_3Nb cannot be. (In the latter case tetragonal distortion lowers the observed DO_{22} lattice by about 1 eV per formula unit compared to the cubic $L1_2$ lattice.)

What is the origin of the oscillations in Φ_3? We see in figure 6 that the Miedema 'macroscopic atom' model does not predict such rapid variations across the series (Carlsson 1989). The beauty of the linearized bond order potential is that it provides for the first time a cluster expansion which is applicable to any lattice and chemical ordering (cf. equations (2.8) and (2.26)–(2.30)).

To understand the quantum mechanical origin of Φ_3 in the transition metal aluminides, let us consider the simpler case of transition metal intermetallics A_cB_{1-c} where the A and B atoms are characterized by atomic d energy levels $-\frac{1}{2}\Delta E$ and $+\frac{1}{2}\Delta E$ respectively and off-diagonal disorder is neglected. The heat of formation may then be written

$$\Delta H^{\mathrm{dis}} = \Delta H^{\mathrm{dis}}_{\mathrm{vol}} + \Delta H^{\mathrm{dis}}_{\mathrm{bond}}, \tag{3.3}$$

PHILOSOPHICAL TRANSACTIONS OF THE ROYAL SOCIETY A MATHEMATICAL, PHYSICAL & ENGINEERING SCIENCES

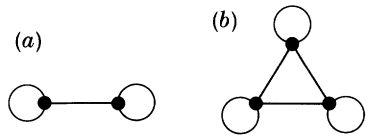

Figure 7. The two-body (*a*) and three-body (*b*) diagrams which contribute to Φ_2 and Φ_3 respectively. The bubbles represent hopping on the same site, which would give a factor $-\frac{1}{2}\Delta E$ ($+\frac{1}{2}\Delta E$) for an A (B) atom.

where $\Delta H^{\rm dis}_{\rm vol}$ is the usual contribution to the heat of formation due to differences in the equilibrium atomic volume of the pure constituents. The contribution from the change in the bond energy may be arranged as

$$\Delta H^{\rm dis}_{\rm bond} = \tfrac{1}{2}(10zh)\left\{\begin{array}{l} 2c(1-c)\,[\Theta^{\rm dis}_{\rm AB} - \tfrac{1}{2}(\Theta^{\rm dis}_{\rm AA} + \Theta^{\rm dis}_{\rm BB})] \\ +[c(\Theta^{\rm dis}_{\rm AA} - \Theta^{\rm A}_{\rm AA}) + (1-c)\,(\Theta^{\rm dis}_{\rm BB} - \Theta^{\rm B}_{\rm BB})]\end{array}\right\}, \tag{3.4}$$

where, for simplicity, the explicit σ, π, and δ bond character has been averaged out in an effective bond integral $h < 0$ (see, for example, p. 80 of Pettifor 1987) and the prefactor 10 accounts for the d band degeneracy. $\Theta^{\rm dis}_{\rm AB}$, $\Theta^{\rm dis}_{\rm AA}$, and $\Theta^{\rm dis}_{\rm BB}$ are the bond orders of the AB, AA, and BB bonds in the disordered A_cB_{1-c} alloy respectively, whereas $\Theta^{\rm A}_{\rm AA}$ and $\Theta^{\rm B}_{\rm BB}$ are the bond orders of the AA and BB bonds in pure A and pure B respectively.

The response functions describing the AB and the average of the AA and BB bond orders in the disordered alloy are the same, as both are determined by the average of the moments about sites A and B through (2.17) and (2.20)–(2.24). Thus, neglecting the change in the AA and BB bond orders in going from the elemental metals to the alloy, (3.4) for the heat of formation may be written as

$$\Delta H^{\rm dis}_{\rm bond} = 20z|h|\,c(1-c)\left\{\sum_{n=0}^{\infty}\chi^{\rm dis}_{0n,\,n0}\,\Delta[\delta a_n] + 2\sum_{n=1}^{\infty}\chi^{\rm dis}_{0(n-1),\,n0}\,\Delta[\delta b_n]\right\}, \tag{3.5}$$

where
$$\Delta[\delta a_n] = [\delta a_n]_{\rm AB} - [\delta a_n]_{({\rm AA}+{\rm BB})/2} \tag{3.6}$$

and
$$\Delta[\delta b_n] = [\delta b_n]_{\rm AB} - [\delta b_n]_{({\rm AA}+{\rm BB})/2}. \tag{3.7}$$

The heat of formation, therefore, depends on those diagrams which are different between the AB and the average AA and BB bond orders. It follows from (2.26)–(2.30) that within the RA the first two nearest-neighbour terms in the cluster expansion are

$$\begin{aligned}\Delta H^{\rm dis}_{\rm bond} = 20z|h|\,c(1-c)\,\{&2(h/b)\,(\Delta E/2b)^2\,\hat{\chi}_4[\tfrac{1}{2}(N_{\rm A}+N_{\rm B})] \\ &+2(1-2c)\,(h/b)^2\,(\Delta E/2b)^3\,\hat{\chi}_6[\tfrac{1}{2}(N_{\rm A}+N_{\rm B})]\},\end{aligned} \tag{3.8}$$

which correspond to the two diagrams shown in figure 7. $\hat{\chi}_4$ and $\hat{\chi}_6$ are functions of the average number of valence electrons per spin per AB bond, namely $\frac{1}{2}(N_{\rm A}+N_{\rm B})$.

The two-body and three-body cluster interactions are given by comparing (3.2) and (3.8). Assuming a rectangular density of states of width W for which $|b| = \mu_2^{\frac{1}{2}} = W/\sqrt{12}$ and a close-packed lattice for which $z = 12$, we have

$$\Phi_2 = -5\sqrt{3}\,W(\Delta E/W)^2\,\hat{\chi}_4 \tag{3.9}$$

and
$$\Phi_3 = -\tfrac{5\sqrt{3}}{2}W(\Delta E/W)^3\,\hat{\chi}_6. \tag{3.10}$$

This predicted behaviour of Φ_2 and Φ_3 as a function of the average number of valence electrons per AB bond is similar to that found computationally using the

Connolly–Williams method for transition metal intermetallics (see fig. 1*a* of Sluiter & Turchi 1989) and for the transition metal aluminides in figure 6 (Carlsson 1989). We see, therefore, that the rapid oscillations in Φ_3 are real, reflecting the wave mechanical nature of the three-body diagram in figure 7.

4. Conclusion

We have shown that the theoretically derived bond order potentials should be invaluable for the atomistic simulation of intermetallics where both the angular character and the many-body nature of the potential are important. We illustrated this for the case of metals with negative Cauchy pressure which in the past could not be treated realistically by other available potentials (see, for example, Johnson 1988). In addition we demonstrated that the very important deviations from regular solution behaviour are a direct consequence of an explicit three-body term in a newly derived cluster expansion. It remains to apply these bond order potentials to specific systems such as FCC iridium or $L1_2$ Al_3Ti in order to explore the possible microscopic mechanisms which may be responsible for their unexpected brittleness.

We thank the U.S. Department of Energy, Energy Conversion and Utilization Technologies (ECUT) Materials Program, for financial support under subcontract no. 19X-55992V through Martin Marietta Energy Systems Inc. D.G.P. acknowledges Dr C. T. Liu of the Oak Ridge National Laboratory for his continuing enthusiasm and support for a more fundamental understanding in alloy design.

References

Aoki, K. & Izumi, O. 1979 Improvement in room temperature ductility of the $L1_2$ type intermetallic compound Ni_3Al by boron addition. *Nippon Kinzoku Gakkaishi* **43**, 1190–1195.

Aoki, M. & Pettifor, D. G. 1991 (In preparation.)

Carlsson, A. E. 1989 Cluster interactions and physical properties of Al-transition metal alloys. *Phys. Rev.* B **40**, 912–923.

Dimiduk, D. M. & Miracle, D. B. 1989 Directions in high temperature intermetallics research. *Mater. Res. Soc. Symp. Roc.* **133**, 349–359.

Fu, C. L. 1991 Electronic, elastic and fracture properties of trialuminide alloys: Al_3Sc and Al_3Ti. (In the press.)

Haydock, R., Heine, V. & Kelly, M. J. 1972 Electronic structure based on the local atomic environment for tight-binding bands. *J. Phys.* C **5**, 2845–2858.

Johnson, R. A. 1988 Analytic nearest-neighbour model for fcc metals. *Phys. Rev.* B **37**, 3924–3931.

Nicholson, D. M., Stocks, G. M., Temmerman, W. M., Sterne, P. & Pettifor, D. G. 1989 Structural energy differences in Al_3Ti: the role of tetragonal distortion in APB and twin energies. *Mater. Res. Soc. Symp. Proc.* **133**, 17–22.

Pettifor, D. G. 1983 Electron theory of metals. *Physical metallurgy* (ed. R. W. Cahn & P. Haasen), pp. 73–152. Amsterdam: Elsevier.

Pettifor, D. G. 1987 A quantum-mechanical critique of the Miedema rules for alloy formation. *Solid St. Phys.* **40**, 43–92.

Pettifor, D. G. 1988 Structure maps for pseudobinary and ternary phases. *Mater. Sci. Technol.* **4**, 675–691.

Pettifor, D. G. 1989 New many-body potential for the bond order. *Phys. Rev. Lett.* **63**, 2480–2483.

Pettifor, D. G. 1990 From exact to approximate theory: the Tight Binding Bond model and many body potentials. *Springer Proc. Phys.* **48**, 64–84.

Pettifor, D. G. 1991 It's all very well in practice but what about in theory? *New materials for the next century: a scientific, technological and industrial revolution* (ed. G. A. D. Briggs). Oxford: Blackwells.

Schneibel, J. H. & Porter, W. D. 1989 Microstructure and mechanical properties of $L1_2$-structure alloys based on Al_3Zr. *Mater. Res. Soc. Symp. Proc.* **133**, 335–340.

Sluiter, M. & Turchi, P. 1989 Electronic theory of phase stability in substitutional alloys: a comparison between the Connolly–Williams scheme and the generalized perturbation method. *Alloy phase stability* (ed. G. M. Stocks & A. Gonis), pp. 521–528. Dordrecht: Kluwer.

Subramanian, P. R., Simmons, J. P., Mendiratta, M. G. & Dimiduk, D. M. 1989 Effect of solutes on phase stability in Al_3Nb. *Mater. Res. Soc. Symp. Proc.* **133**, 51–56.

Discussion

J. N. Murrell (*University of Sussex, U.K.*). The concept of bond order is not sufficiently well defined outside the simplest systems (e.g. organic hydrocarbons) for this to form the basis of quantitatively successful theories. The reason for this is that bond orders for, say, triangles of different side lengths, are not unambiguously defined.

D. G. Pettifor. The simple two-centre, orthogonal tight binding Hückel theory has been shown to predict successfully the trends in crystal structure of elemental systems through the periodic table, of binary intermetallics through the AB, AB_2, and AB_3 structure maps, and of small microclusters of carbon and silicon. The many-body potential for the bond order is derived directly from this TB model and, therefore, is well based to predict trends in structural behaviour.

A. Cottrell (*Department of Materials Science, Cambridge, U.K.*). To avoid brittleness I think a short Burgers vector is needed, i.e. not a superlattice vector. This means that the two atoms in the intermetallic have to be fairly indifferent towards one another, which implies a modest melting point. That from the practical point of view is a depressing conclusion, but it might be possible to bypass it with a disordered intermetallic. Does Professor Pettifor have a view on this?

D. G. Pettifor. My only comment is that the well-known ductilization of Ni_3Al polycrystals by adding boron appears to be due to the boron attracting excess nickel to the grain boundary, thereby setting up a disordered layer which improves the mechanical properties. We have still to perform atomistic simulations of crack tips in elemental and binary metals with these new angularly dependent bond order potentials, and to study the influence of ordering energy on the mechanical response.

A. M. Stoneham (*Harwell, U.K.*). Professor Pettifor has used a non-self-consistent approach; for metals, one can see this could work, but for semiconductors (where defect charge state matters, e.g. in Fermi level effects on dislocation motion) surely more is required?

D. G. Pettifor. Yes, of course.

PHILOSOPHICAL TRANSACTIONS OF THE ROYAL SOCIETY A MATHEMATICAL, PHYSICAL & ENGINEERING SCIENCES